Agricultural Water Management 255 (2021) 107010

Contents lists available at ScienceDirect

Agricultural Water Management

journal homepage: www.elsevier.com/locate/agwat

Water-use patterns of Chinese wolfberry (*Lycium barbarum* L.) on the Tibetan Plateau

Yanqing Zhou [a,c], Xiaodong Gao [b,*], Jiaxin Wang [a], Brett H. Robinson [d], Xining Zhao [b,*]

[a] College of Water Resources and Architectural Engineering, Northwest A & F University, Yangling 712100, China
[b] Institute of Soil and Water Conservation, Northwest A & F University, Yangling 712100, China
[c] State Key Laboratory of Desert and Oasis Ecology, Xinjiang Institute of Ecology and Geography, Chinese Academy of Sciences, Urumqi 830011, China
[d] School of physical and Chemical Sciences, University of Canterbury, Christchurch 8140, New Zealand

ARTICLE INFO

Handling Editor - Dr. B.E. Clothier

Keywords:
Chinese wolfberry
Water use strategy
Stable isotope
Bayesian mixing model
Water use efficiency

ABSTRACT

Chinese wolfberry (*Lycium barbarum* L.) can efficiently ameliorate land deterioration and increase farmers' incomes on the Tibetan Plateau. Therefore, it has been widely grown in this region in the past decades. The aims of this study were to clarify the patterns of water sources and water use efficiency under 3 management practices to determine the optimal cultivation strategies. A 2-year field experiment was undertaken in a Chinese wolfberry plantation with 3 management practices, including the conventional flat planting plus surface drip irrigation (CK), flat planting with full-film mulching plus surface drip irrigation (MF) and ridge-furrow full-film mulching plus surface drip irrigation (MR). The soil moisture in shallow (0–20 cm), middle (20–60 cm) and deep (60–100 cm) soil layers were regarded as the trees' potential water sources. The IsoSource model and two Bayesian mixing models of MixSIR and MixSIAR were employed to calculate the contribution of different water sources to xylem water. The MixSIR model exhibited relatively better performance in quantifying water source contribution for different layers compared with the IsoSource and MixSIAR models. Management practices significantly altered water use patterns of the wolfberry during the growing periods. Under CK the wolfberry preferentially extracted moisture from the middle and deep layers even during rainfall and irrigation. Under MF and MR they switched more flexibly their water source between the three layers; and they used more water from shallow and middle layers when soil moisture availability increased there, which was especially true under MR. Compared with CK, the average yield of MR and WUE were found to increase by 21.5% and 17%, respectively, over the 2-years period. This indicated that film mulching and ridge-furrow altered the water use strategy of Chinese wolfberry and WUE, which can inform the designing of the best management regimes. The response to tree water use in terms of soil nutrients and subsurface irrigation should be investigated to optimize field management practices, including irrigation schedules and modes.

1. Introduction

The Tibetan plateau (TP), often called the 'Third Pole', plays a major role in safeguarding the environmental security downstream in East China and South Asia (Yao et al., 2012). Moreover, the ecological environment on the Qinghai-Tibet Plateau is extremely sensitive to human activities. However, land uses on the TP have been extensively transformed by socio-economic development and intensifying human activity, especially overgrazing (Wang et al., 2020a; Wu et al., 2021). This has led to severe socio-economic and ecological problems, including increasing desertification, grassland degradation and reduction in forest cover (Cao et al., 2004; Chen et al., 2011; Feng et al., 2005; Jin et al., 2019; Miehe et al., 2019). In the past decades, the Chinese government has adopted several measures to recover and protect the degraded rangelands (Chen et al., 2021; Wu et al., 2021), including enclosure, closure against grazing and reducing livestock density (Wu et al., 2021). However, a consensus on the magnitude of efforts to be made in these measures is lacking, although these measures are directly linked to the improvement of farmer's incomes. Developing high value-added ecological agriculture may ameliorate the degradation by reducing overgrazing and improving livelihoods of the farmers and herders (Jin et al., 2019; Miehe et al., 2008, Zhou et al., 2019).

Chinese wolfberry (*Lycium barbarum* L.), also called the goji berry, hereafter wolfberry, is a crop of high economic value that has been

* Corresponding authors.
E-mail addresses: gao_xiaodong@nwafu.edu.cn (X. Gao), zxn@nwafu.edu.cn (X. Zhao).

https://doi.org/10.1016/j.agwat.2021.107010
Received 28 September 2020; Received in revised form 3 June 2021; Accepted 4 June 2021
Available online 15 June 2021

widely used to ameliorate wind erosion and improve soil structure. The northern part of the TP provides suitable conditions for its cultivation (abundant sunshine and large diurnal temperature variation), and has become the second largest area (after the Ningxia Hui Autonomous Region) for its production in China (Lei et al., 2020). However, drought and water scarcity have strongly constrained development of wolfberry orchards on the TP (Deng et al., 2017; Xu et al., 2019). Therefore, minimising water use and enhancing water productivity are essential. Mulching and drip irrigation are among the well-known approaches (Mo et al., 2017; Liao et al., 2019a, 2019b, 2021; Fang et al., 2021). The subsurface irrigation method has been applied in the arid and semi-arid areas of China in recent years considering that it has near-zero soil evaporation and optimum nutrient supply (Cai et al., 2021; Fu et al., 2021). In this area, the irrigation system should be upgraded from the surface drip irrigation method to the subsurface drip irrigation method. Therefore, the water uptake patterns of wolfberries during the growth period should be elucidated to formulate an optimal water management system and the best-buried depth for the subsurface drip irrigation.

Analysis of stable hydrogen and oxygen isotopes provides a highly sensitive and accurate approach to study plants' water use patterns and eco-hydrological processes (Barbeta and Penuelas, 2017; Dai et al., 2015; Dawson and Ehleringer, 1991; Huo et al., 2018; Gao et al., 2018a; Grossiord et al., 2017; Wang et al., 2020b), especially in the arid and semi-arid areas (Wu et al., 2016; Wu et al., 2018; Gao et al., 2018b; Yang et al., 2015; Zhao et al., 2016). The theoretical basis is that xylem water can be regarded as a mixture of water from all utilized sources, so the proportional uses of specific sources can be estimated by comparing hydrogen or oxygen isotope signatures of xylem water and all potential water sources (Dawson et al., 2002; Huo et al., 2018). These analyses assume that no fractionation of these isotopes occur during root water uptake except in halophytic and xerophytic plants (Ellsworth and Williams, 2007; Lin and Sternberg, 1993). However, recent studies reported that deuterium fractionation in root water uptake may occur even for trees in the temperate oceanic climate (Barbeta et al., 2018). On the contrary, there are no reports according to our knowledge on the fractionation of stable oxygen isotopes. Therefore, in the present study we have used stable oxygen isotopes to measure water use patterns of wolfberry.

End-member mixing models are widely used to quantify water sources across global ecosystems. They can be categorised as simple linear mixing models (e.g., IsoSource) and Bayesian mixing models (e.g., MixSIR and MixSIAR) (Rothfuss and Javaux., 2017). Unlike the former, Bayesian mixing models incorporate uncertainties of prior information in data processing (Stock et al., 2018; Wang et al., 2019). In most published studies of plants' water use patterns, only one of these two kinds of models has been used. However, Evaristo et al. (2017) recently found that the two-source mass balance model over-estimated the groundwater contribution to trees' xylem water in Christchurch Botanic Gardens, New Zealand. Differences in results of the two kinds of mixing models have rarely been tested in other ecosystems. Therefore, the objectives of this study were to quantify the variation in water use patterns of wolfberry trees on the TP using oxygen stable isotopes, and both simple and Bayesian mixing models, to obtain sound foundations for water management and crop production in wolfberry orchards.

2. Materials and methods

2.1. Site description

The study was conducted in the Huaitou Tala Irrigation Area (37° 21′ N, 96° 44′ E; 2869 m above sea level), in the northeastern part of the TP in Haixi Mongol and Tibetan Autonomous Prefecture. It has a typical continental climate for the plateau: dry, windy and cold. According to reference data for the period 1977–2016 collected at Delingha weather station, annual minimum, average and maximum air temperatures are − 27.9, 6.5 and 34.7 °C, respectively. Mean annual precipitation amounts to just 241 mm, of which more than 70% occurs from June to September. Accordingly, the area receives abundant sunshine (3010 h per year on average). The groundwater depth exceeds 50 m. According to the International Soil Classification System, the local soil type belongs to sandy loam, the soil texture is about 82% sand (0.02–2 mm) in the 0–100 cm layer. Basic properties of the soil in the study area are shown in Table 1.

2.2. Experimental design

The study was conducted in a wolfberry orchard where the trees were planted, with 1 m × 3 m, spacing in 2015. Drip irrigation was applied, with 50 cm spacing of drippers, each supplying 3.75 l h^{-1} for six times in 4 h during the growth period and then once in winter after defoliation (for approximately 10 h). Because the study area was a demonstration area of the best irrigation and fertilization system of wolfberry in the alpine region (Li, 2019), we followed the local irrigation schedule. Three treatments were applied in the orchard: conventional flat planting plus surface drip irrigation (CK), flat planting with full-film mulching plus surface drip irrigation (MF) and ridge-furrow full-film mulching plus surface drip irrigation (MR) in 1.5 m × 20 m plots, with 1.5 m buffers, in a randomised block design; each plot comprised 20 trees, with 3 replicates per treatment. On each sampling occasion, one tree in each plot was randomly selected. A black gardening cloth was used in this study. The ridges and furrows had the same width, which is 20 cm, and the ridge height is 30 cm, and the wolfberry planted in the ditch. Similar planting patterns can be found in Gu et al. (2016). Uniform summer pruning, pest and disease control, and fertiliser supply were carried out for all treatments.

2.3. Fine root sampling

In October 2018 samples of the 0–120 cm soil layer were taken (at 20,40, 60, 80,100, 120 cm depth) from three equally spaced points 0.3 m away from the trunk of each of one wolfberry trees in each plot. Taking into account the influence of wolfberry canopy expansion and root growth. Root samples were collected at 0–100 cm (no sample at 120 cm) soil layer from the wolfberry trees trunk (three equally spaced points) at 0.3 and 0.6 m radial distance in October 2019. The samples were collected using a hand auger (90 mm diameter), and passed through a 2 mm sieve to separate gravel from the soil. Roots were removed with tweezers, eliminating dead roots and grass roots. And a vernier caliper with 1×10^{-2} precision was used to take fine roots (≤ 2 mm) from root samples. The fine root length density (FRLD) in each case were then calculated:

$$FRLD = length / V \quad (2-1)$$

where length was the fine root length and V was the volume of soil. as described in detail by Li et al. (2017).

2.4. Isotope data acquisition

During growing stages (15 May to 1 October), precipitation and irrigation water samples were taken. The precipitation samples were collected in 600 ml plastic bottles through a 10 cm diameter funnel, with a ping-pong ball placed in the funnel to prevent evaporation, then immediately transferred into 20 ml vials sealed with a cap and Parafilm after rain, samples were subsequently stored in a refrigerator (4 °C) until isotope analysis. Soil and xylem samples were taken in four growth stages: leaf emergence (LFE; mid-May to mid-June), blossom and young fruit (BYF; late June to mid-July), fruit maturation (FTM; late July to mid-September) and defoliation (DF; late September to early of October) after a period of at least 5 days with no rainfall or irrigation. The sampling dates were 9 July, 30 July and 22 September in 2018 and 6 June, 18 July, 16 August and 1 October in 2019. In each plot, wolfberry trees

Table 1
Soil physical properties and soil available nutrients in the study site.

Soil depth (cm)	Bulk density ($g \cdot cm^{-3}$)	Saturated water content (vol%)	Total N ($g \cdot kg^{-1}$)	Available N ($mg \cdot kg^{-1}$)	Available P ($mg \cdot kg^{-1}$)	Available K ($mg \cdot kg^{-1}$)	Humus ($k \cdot kg^{-1}$)
0–20	1.56 ± 0.07	22.1 ± 1.44	0.36 ± (0.43%)	41.47 ± 0.32	55.28 ± 0.47	89.31 ± 2.14	1.09 ± 0.32
20–40	1.54 ± 0.09	24.43 ± 0.84	0.33 ± (0.38%)	51.12 ± 0.56	19.61 ± 0.6	82.22 ± 0.91	1.33 ± 0.03
40–60	1.5 ± 0.05	31.67 ± 0.43	0.28 ± (0.15%)	35.56 ± 0.64	17.05 ± 1.08	47.11 ± 0.66	2.04 ± 0.05
60–80	1.52 ± 0.04	27.25 ± 0.72	0.25 ± (0.19%)	57.84 ± 0.85	15.92 ± 0.61	34.53 ± 0.65	1.77 ± 0.04
80–100	1.5 ± 0.07	29.12 ± 0.65	0.27 ± (0.14%)	69.12 ± 1.22	14.27 ± 0.47	33.42 ± 0.97	1.5 ± 0.06

with similar mean heights and ground diameters were selected for sampling (Table 2). On each sampling occasion, one of these trees in each plot was randomly selected, then soil and xylem samples were simultaneously collected. Three lignified branches were cut from the sunny side, and cut into 1–2 cm pieces, from which bark and phloem were removed to prevent possible isotope fractionation of xylem water (Huo et al., 2018). Samples were then immediately placed in vials, which were wrapped in parafilm and put in a portable cooler to avoid evaporation. Samples of 0–10, 10–20, 20–40, 40–60, 60–80 and 80–100 cm soil layers were also collected from each tree using a hand auger (Φ = 40 mm) at a distance of 30 cm away from the trunk.

Every layer of soil samples were mixed well and divided into two parts, one of which was placed in wrapped vials, like the xylem samples, while the other was placed in a soil moisture tin and sealed for subsequent gravimetric determination of soil water content. All the xylem and soil samples were transported to the laboratory and stored in a freezer (−15 ℃–−20 ℃) before water extraction. Each sampling event was between 8:30 and 12:00 when the trees were transpiring. In addition, meteorological information (rainfall, net radiation, air temperature, etc.) during the study period was recorded by an AR5 weather station located 50 m north of the orchard.

2.5. Determination of stable isotopic composition

The water was extracted from the xylem samples and the soil samples, by an LI-2000 cryogenic vacuum distillation system (Los Gatos Research, Mountain View, USA) and placed in 5 ml glass vials sealed with Parafilm, which were stored at 4 °C until isotope analysis. The oxygen isotope composition of the water extracted from the soil samples was measured using a TIWA-45EP Isotopic Ratio Infrared Spectroscopy (IRIS) analyser (Los Gatos Research, Mountain View, USA), which provides analytical precision of ± 0.2‰ for $\delta^{18}O$. To avoid any effects of organic compounds in the samples of cryogenically extracted xylem water, they were measured using an Isotope Ratio Mass Spectrometry (TRMS), which provides the same analytical precision with IRIS for $\delta^{18}O$.

2.6. Fruits yield and WUE

Natural precipitation and irrigation represent the main source of Chinese wolfberry water in the study area. Chinese wolfberry mainly consumes water from soil moisture, precipitation and irrigation during the growth period. Thus, the water balance equation is:

$$ET = P + I + \Delta W - R - D - G \quad (2\text{-}2)$$

where ET is evapotranspiration during the growth period, P is the precipitation during the same period, I is irrigation, ΔW is variation in the soil water storage in the 0–100 cm layer between the beginning and end of the growth period, R is runoff, D is leakage and G is capillary-lifted water. The underground water level in the study area was < 50 m. The leakage (D) and capillary water (G) can therefore be neglected. A small magnitude of precipitation during the growth period ensured that the runoff (R) was also negligible. The water balance equation can thus be modified as follows:

$$ET = P + I + \Delta W \quad (2\text{-}3)$$

The total fruit yield at maturity were weighed in each treatment method separately, and WUE (kg ha^{-1} mm^{-1}) was calculated using the following equation:

$$WUE = Yield/ET \quad (2\text{-}4)$$

where yield is the fruit yield at wolfberry harvest (kg ha^{-1}), and ET is the total evapotranspiration (mm).

Table 2
Mean heights and ground diameter (with standard deviations) of the Chinese wolfberry stands in the plots subjected to each of the treatments.

Treatment	Height (cm)	Ground diameter (mm)	Planting density
CK	123 ± 5.90	29.33 ± 0.64	1 m × 3 m
MF	116 ± 4.70	27.89 ± 0.51	1 m × 3 m
MR	110 ± 3.48	30.89 ± 1.10	1 m × 3 m

2.7. Data analysis

2.7.1. Determination of plant water sources partitioning methods

We used three approaches (one linear mixing model (IsoSource) and two Bayesian models (MixSIR and MixSIAR)) to determine contributions of water sources for the wolfberry trees. The first method was application of the simple IsoSource mixing model to obtain feasible ranges of water sources used by the plants (Phillips and Gregg, 2003). Based on the distributions $\delta^{18}O$ values and fine root length density (FRLD), we considered three potential water sources: shallow (0–20 cm), middle (20–60 cm) and deep (60–100 cm) soil layers. These layers were expected to have distinct characteristics. The isotopic composition of the soil water in the top 20 cm generally fluctuates most due to precipitation and evaporation, and shallow layers have higher FRLD than the middle and deep layers. The deep soil layers relatively stable isotopically and have low FRLD. The middle layer was expected to have intermediate isotopic fluctuation. In the IsoSource model, the source increment was set at 1% and the mass balance tolerance at 1% (2% when use of 1% was fruitless), the result is described by the distribution of all such feasible solutions (Table S1). The mean value of isotopic values in plant xylem and the potential water sources were considered when the IsoSource model was run. In the second approach, we used Bayesian mixing models (MixSIR) with sampling importance resampling algorithm, which explains uncertainties associated with multiple sources. The MixSIR model can add prior knowledge. The mean $\delta^{18}O$ and their standard deviations (SD) values of xylem samples and source isotope compositions were input into the model. The third was used the Bayesian mixing models (MixSIAR, the posterior distribution use the Markov chain Monte Carlo sampling technique) includes the advantages of MixSIR, in addition, MixSIAR model can also explain variation in proportional contributions of sources through fixed and random effects (Stock et al., 2018). Inputs for the MixSIAR model included means and standard deviations of isotopic values for plant xylem and each potential water source. The concentration dependence and TEF (trophic enrichment factor) values were set to zero. the MixSIAR model with “long” or “very long” settings, until convergence. More detailed information regarding the parameters of those models can be found in Wang et al.

(2019). The output result of the IsoSource model is the frequency and range of the contribution of potential water sources, to evaluate the performance of the IsoSource model, we used the average contribution rate (frequency) of potential water sources. The output of the Bayesian models (MixSIR and MixSIAR) is the average contribution rate of potential water sources rather than the frequency distribution of the feasible solution.

2.7.2. Evaluation of model performance

It is difficult to obtain measure directly the water source contributions to plants (Rothfuss and Javaux, 2017). Therefore, we indirectly evaluated the prediction effect of different water source allocation with different data input models by assessing the degree of match between observed and predicted values of xylem water isotopic compositions (Wang et al., 2019).

In this study, the isotopic compositions of xylem water were considered as the observed values (O_i). The predicted value (p_i) were based on the assumption that the water isotopic compositions of the plant is a mixture of various potential water sources (Ehleringer and Dawson, 1992, Stock et al., 2018). The predicted value p_i was calculated as follows:

$$p_i = \sum_{j=1}^{k} f_j \delta_x \quad (2\text{-}5)$$

where: j represents the j_{th} water source, k is the total number of water sources (there are three water sources in this study, $k = 3$), f refer to the contribution rate of the water source which were predicted by water source partitioning methods, and δ_x represents the isotope value of the water source ($\delta^{18}O$) .

To evaluate the performance of different models, we calculated five indicators as follows:

(1) Root mean square error, RMSE

$$RMSE = \sqrt{\frac{1}{n}\sum_{1}^{n}(p_i - o_i)^2} \quad (2\text{-}6)$$

(2) Nash coefficient, NE

$$NE = 1 - \frac{\sum_{i=1}^{n}(p_i - o_i)^2}{\sum_{i=1}^{n}(o_m - o_i)^2} \quad (2\text{-}7)$$

(3) Mean absolute percentage error, MAPE

$$\text{MAPE} = \frac{1}{n}\sum_{i=1}^{n}\left|\frac{p_i - o_i}{o_i}\right| \quad (2\text{-}8)$$

(4) The maximum prediction error, MaxE

$$MaxE = \max(p_i - o_i) \quad i = 1, \ldots\ldots n \quad (2\text{-}9)$$

(5) The minimum prediction error, MinE

$$MinE = \min(p_i - o_i) \quad i = 1, \ldots\ldots n \quad (2\text{-}10)$$

where: p_i and o_i are the predicted and observed values of water isotope composition in plant xylem; n mean the number of observations, o_m is the average of observed values. Smaller RMSE values indicated less error in the models. A NE value of 1 indicates that the prediction results are completely accurate, the closer NE is to 1, the higher the reliability of the model. MAPE $< 10\%$ indicates high fit; $10\% <$ MAPE $< 20\%$ indicates fine fit; 20%<MAPE< 50% indicates feasible fit; MAPE> 50% means infeasible fitting (Zhang et al., 2020).

2.7.3. Statistical analysis

The data were analysed using SPSS 23.0 software (SPSS Inc., Somers, NY, USA). One-way ANOVA (with post-hoc Duncan tests) was used to analyse between-treatment and between-layer differences in FRLD at the 0.05 probability level. Relationships between soil water contents and both contributions of water sources to the wolfberry trees and FRLD were analysed by linear regression. Figures were drawn using OriginPro 2016 software (OriginLab Corporation, Northampton, MA, USA).

3. Results

3.1. Climate and isotopic composition ($\delta^{18}O$) of rainwater and irrigation water

Daily rainfall, mean air temperature and $\delta^{18}O$ values of rainwater and irrigation water recorded at the study area from May to September in 2018 and 2019 are shown in Fig. 1. The total rainfall during the growing period was 146.8 mm and 130.4 mm in 2018 and 2019, respectively. More than 78% of the rainfall occurred from the beginning of 1st June to 31st August. There were wide variations in both $\delta^{18}O$ values of the rainfall (−14.4 to 1.7‰) and amounts of precipitation throughout the growing period. The Pearson's correlation analysis indicated no correlation between the $\delta^{18}O$ values of rainwater and rainfall or daily average temperature.

3.2. Soil water content and stable isotope composition of soil water

The soil water profiles varied substantially between both treatments and growth stages (Fig. 3). Soil water contents were higher under the MF and MR treatments than under CK, by 30.2% and 37.1%, respectively, on average across the soil profile on the seven sampling occasions. In addition, the water content of shallow soil fluctuated most strongly, and the ranges of soil water content have decreased over soil depth; the water content of deep soil showed slight fluctuations. The change pattern of the $\delta^{18}O$ values of water was similar among the treatments. Therefore, we did not consider differences in the change pattern of the $\delta^{18}O$ values of water across the treatments. The Fig. 4 shows the temporal and spatial variation of soil water $\delta^{18}O$ values under all treatment. The $\delta^{18}O$ values of water in the shallow layer clearly varied. The variations in $\delta^{18}O$ values were lower in the middle layer under each treatment, and no significant variations were detected in the deep layer.

3.3. Seasonal water use patterns of wolfberry under the three treatments

Estimates of relative contributions of water from the three potential sources were obtained from the oxygen isotope values using the IsoSource, MixSIR and MixSIAR models. The three models indicated that the wolfberry under CK used more water from the deep layer with a mean value of 53.1% (26.8–82.8%) during the growth season. In LFE and DF, CK took up correspondingly large proportions of water from the deep layers by 73.9% and 66.7%, respectively, and CK mainly using the water from the middle and deep layers during BYF and FTM. The MF and MR mainly used water from the middle and deep layers during LEF and DF; they could shift their water source among all 3 layers in BYF and FM, but MR used more the shallow and middle layers water (Fig. 5).

The results obtained using the three methods were similar, regarding the main apparent root water uptake depth of wolfberry. However, there were differences in the relative contributions of water sources they indicated. The MixSIR model displayed a higher proportion of middle water sources than the IsoSource and MixSIAR models in most cases. For instance, the MixSIR model indicated that the middle layer had a higher contribution in the BYF and FTM stages under MR than that indicated by the IsoSource and MixSIAR models in 2018. In addition, under MR, the IsoSource model indicated that the middle layers had higher contributions (62.7%) than the MixSIR (48.5%) and MixSIAR (42.4%) models in LEF in 2019. The summary of the performance of water utilization

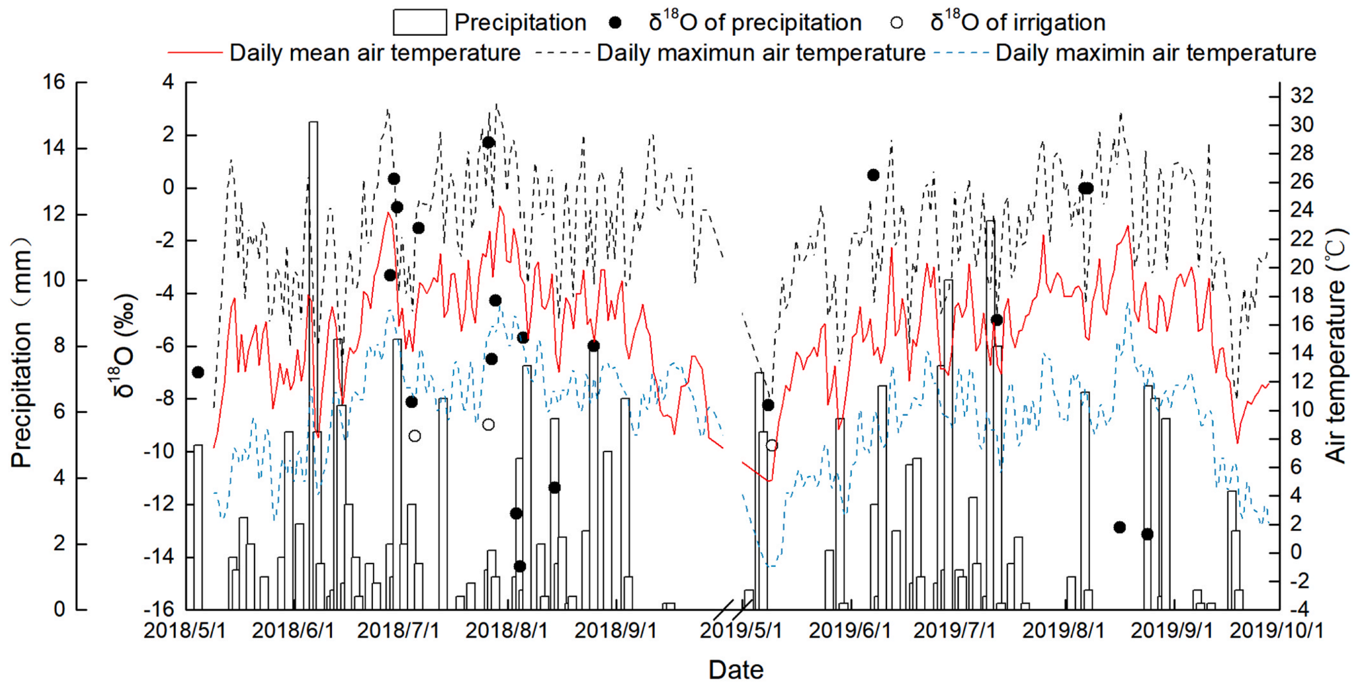

Fig. 1. Temporal variation of amounts and isotopic composition of precipitation and irrigation, and daily temperature, from May to September at the study site in 2018 and 2019.

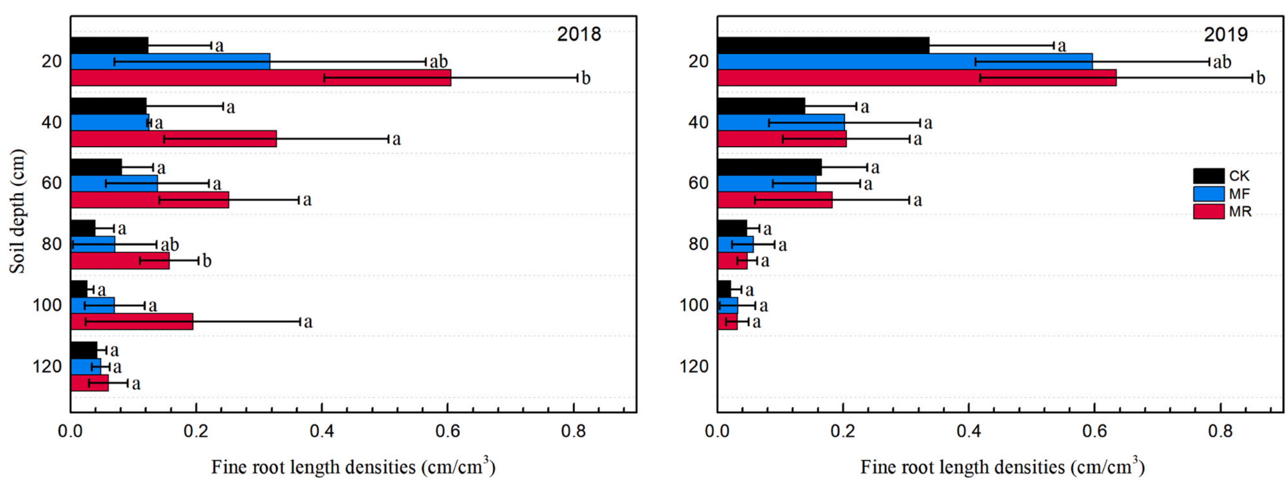

Fig. 2. Vertical distribution of fine root length density (FRLD) with field management in Chinese wolfberry plantation sites. The same letter in different rows indicates that there was no significant difference in FRLD (at $P < 0.05\%$ according to Duncan's test) between corresponding layers for each treatment.

predictions using different models is shown in Table 3. The IsoSource model revealed the lowest RMSE, MAPE MinE and MaxE and the largest NE, which indicated the accuracy and reliability of this model. The RMSE, MAPE and MaxE values of the MixSIAR model were comparatively larger than those of the IsoSource and MixSIR models, while the MixSIAR model showed lower NE values than the IsoSource and MixSIR models, which suggested that the MixSIAR model yields comparatively poorer outcomes in terms of water utilisation prediction.

3.4. Root distributions

The distribution of FRLD under each of the treatments are shown in Fig. 2. The spatial distribution of the roots was influenced by the ridge-furrow system and mulch. Under each treatment condition, most of the fine roots were found in the shallow and middle layers (82.8%, 83.4% and 83.5% of the total roots on an average over 2 years in the CK, MF and MR, respectively). In general, the order of FRLD with different treatments was MR > MF > CK. Although no obvious differences were found in the distribution of FRLD in each treatment group, FRLD of MF and MR were extended compared with that of CK. FRLD in CK within the shallow soil layer was significantly lower than that in MF and MR.

3.5. Yield and WUE

MF and MR showed an increase in yield by 4.7% and 16.4% in 2018 and by 14.4% and 26.6% in 2019, respectively, compared with CK (Table 4). Similar trends were observed in WUE across the treatment groups. Compared with CK, MF and MR improved WUE by 5.7% and 17.1% in 2018 and by 4.2% and 17.0% in 2019, respectively. The maximum yield and WUE value were recorded in MR, whereas the lowest yield and WUE value were recorded in CK.

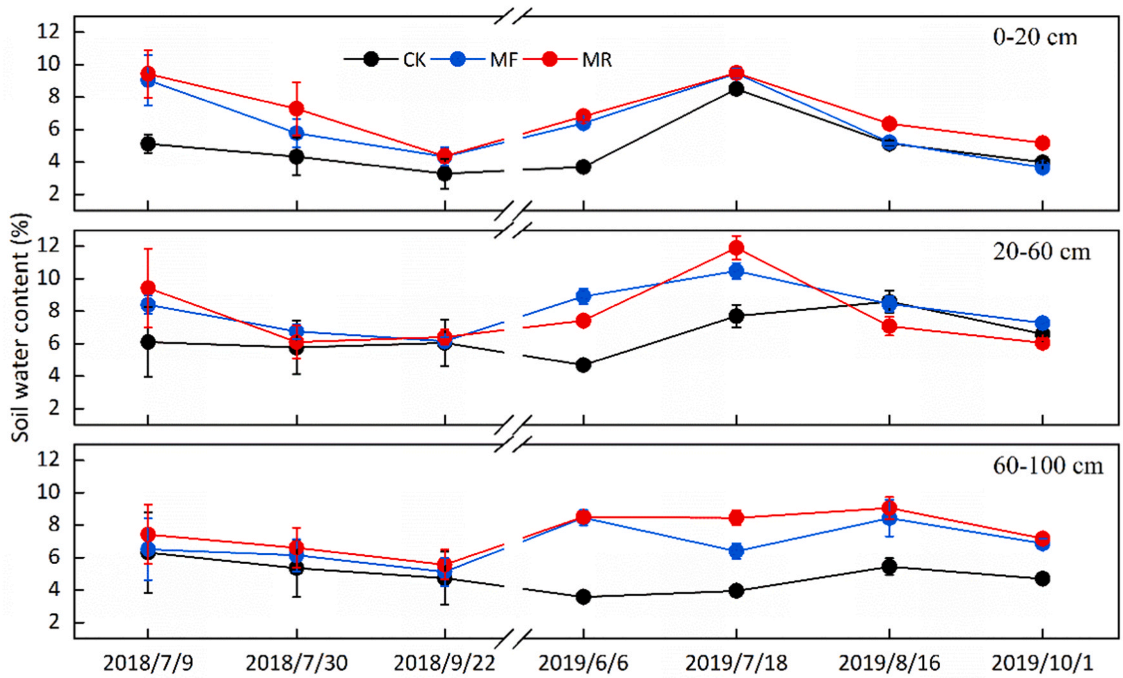

Fig. 3. Temporal and spatial variation of soil water content in the wolfberry orchard under each treatment.

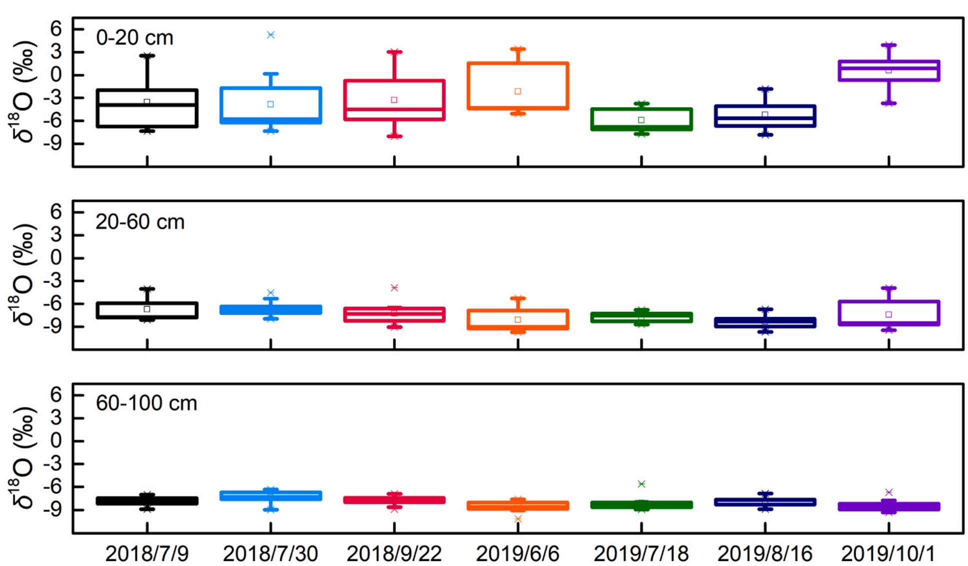

Fig. 4. Temporal and spatial variation of soil water $\delta^{18}O$ values under each treatment. Note: The top and bottom ends of the rectangle are the upper and lower quartiles respectively, the horizontal line in the rectangular frame represents median, the small box represents the mean, and the points outside the rectangle represent outliers.

3.6. Relationship between source contribution and soil water content and fine roots

To understand the effect of the soil water content on root water uptake, we examined correlations between soil layers' contributions to the trees' xylem water and their water contents, using data obtained for all plants at each sampling date. Overall, there was no significant correlation between these variables (Fig. 6). However, water content was positively correlated with the contribution of the shallow layer, but not correlated with the contribution of the middle and deep layers (Fig. 6).

To study the relationship between root water uptake and fine root density, the contribution of each layer to the xylem water of all sampled trees subjected to the same treatment were averaged, to obtain a mean value for each treatment and sampling date. Correlations between these means and proportion of fine biomass (FRLD) values of corresponding soil layers on corresponding sampling dates were then examined. The contribution of water sources decreased exponentially with increases in FRLD when using data obtained for all samples (Fig. 7). Conversely, the contribution of water sources decreased first and then increased with increasing FRLD in the deep layer (Fig. S1). However, there was no significant relationship between the proportion of fine biomass and contribution of water source in shallow and middle layers (Fig. S1).

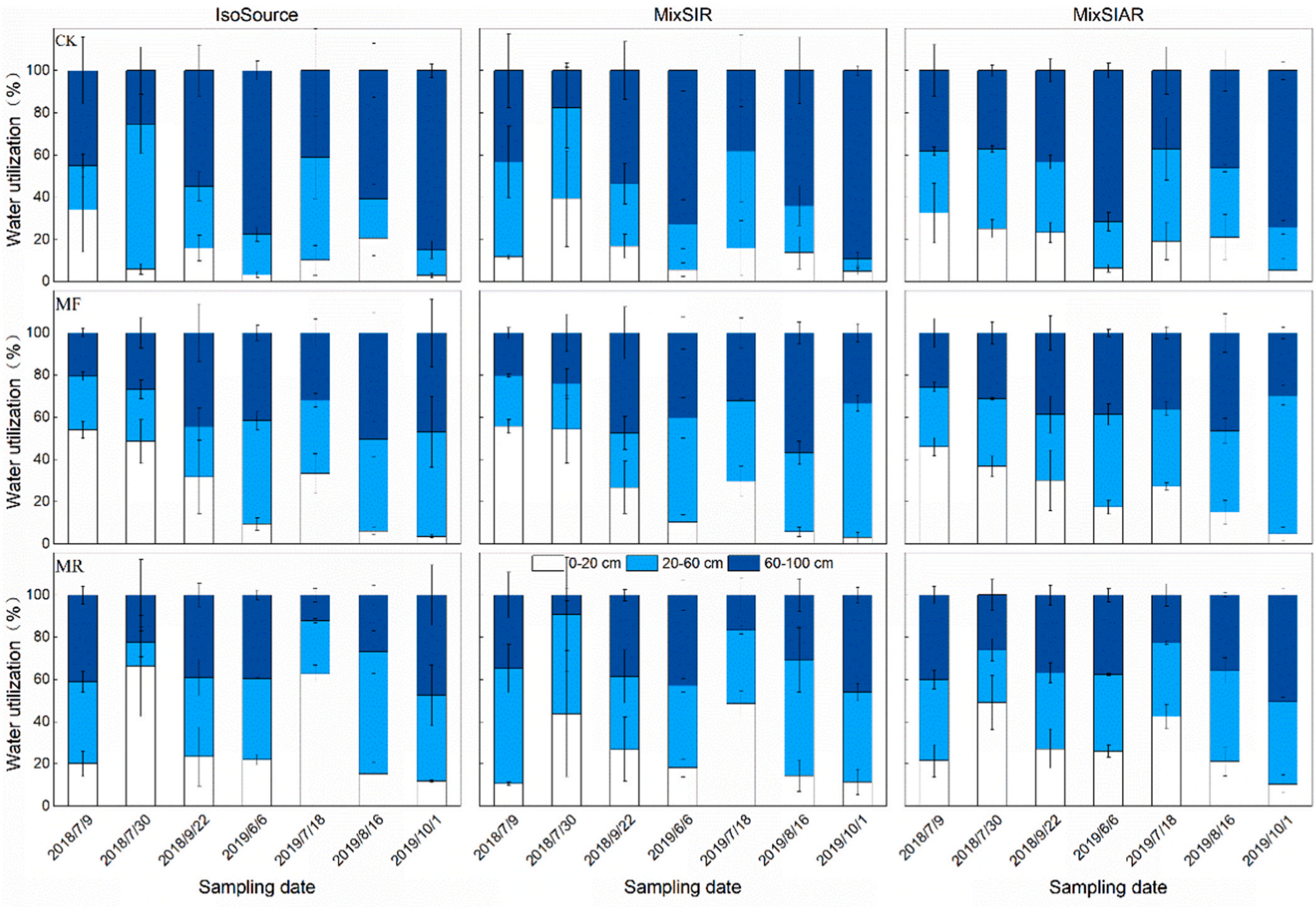

Fig. 5. Temporal variation in contributions of the three soil layers to wolfberry root water uptake under each treatment according to the IsoSource and Bayesian mixing models (MixSIR and MixSIAR).

Table 3
Evaluation of prediction performance on different models.

Evaluation index	IsoSource	MixSIR	MixSIAR
RMSE	0.2025	0.3323	0.5306
NE	0.9634	0.8864	0.7877
MAPE	0.0115	0.0333	0.0609
MaxE	1.0250	1.0632	1.7320
MinE	0.0001	0.0061	0.0038

4. Discussion

4.1. Comparison of different models of water use source identification

The δ^{18}O of the soil water is mainly affected by evaporation and is enriched in the surface layer; however, the effect of evaporation decreases with an increase in soil depth. Therefore, under each treatment, the δ^{18}O of the soil water first decreased rapidly and then tended to be stable with increases in soil depth in the 0–100 cm soil layer, in accordance with previous findings (Cao et al., 2018; Huo et al., 2018; Zhao et al., 2018a). The prediction accuracy of these 3 models was different across different study areas (Evaristo et al., 2017; Wang et al., 2019; Zhang et al., 2020). Therefore, the selection of an accurate prediction model is essential to analyse plant water use patterns. The RMSE values of the models were lower, whereas the NE values of the models were larger than those reported in a study by Wang et al. (2019). These results together indicate that the 3 models had accurate and credible outcomes in the present study. However, some differences in the water uptake proportions were observed among the 3 models. In general, the order of predicting performance was IsoSource > MixSIR > MixSIAR. The best performance of IsoSource was due to the IsoSource model, which did not consider the uncertainties of the stable isotopic composition in plants' water sources and xylem water (Parnell et al., 2010); therefore, the water uptake proportion predictions of the IsoSource model did not necessarily reflect the actual root water absorption (Wang et al., 2019). The Bayesian mixing model (MixSIR and MixSIAR models) can deal with

Table 4
Chinese wolfberry yield and WUE under different treatments.

Year	Treatment	Precipitation (mm)	Irrigation (mm)	Evapotranspiration (mm)	Yield (kg hm^{-1})	WUE (kg hm^{-1} mm^{-1})
2018	CK	146.8	170	318.3	1126.6	3.5
	MF	146.8	170	316.4	1179.9	3.7
	MR	146.8	170	318.1	1312.2	4.1
2019	CK	130.4	170	290.3	1372.7	4.7
	MF	130.4	170	318.7	1571.4	4.9
	MR	130.4	170	313.7	1737.9	5.5

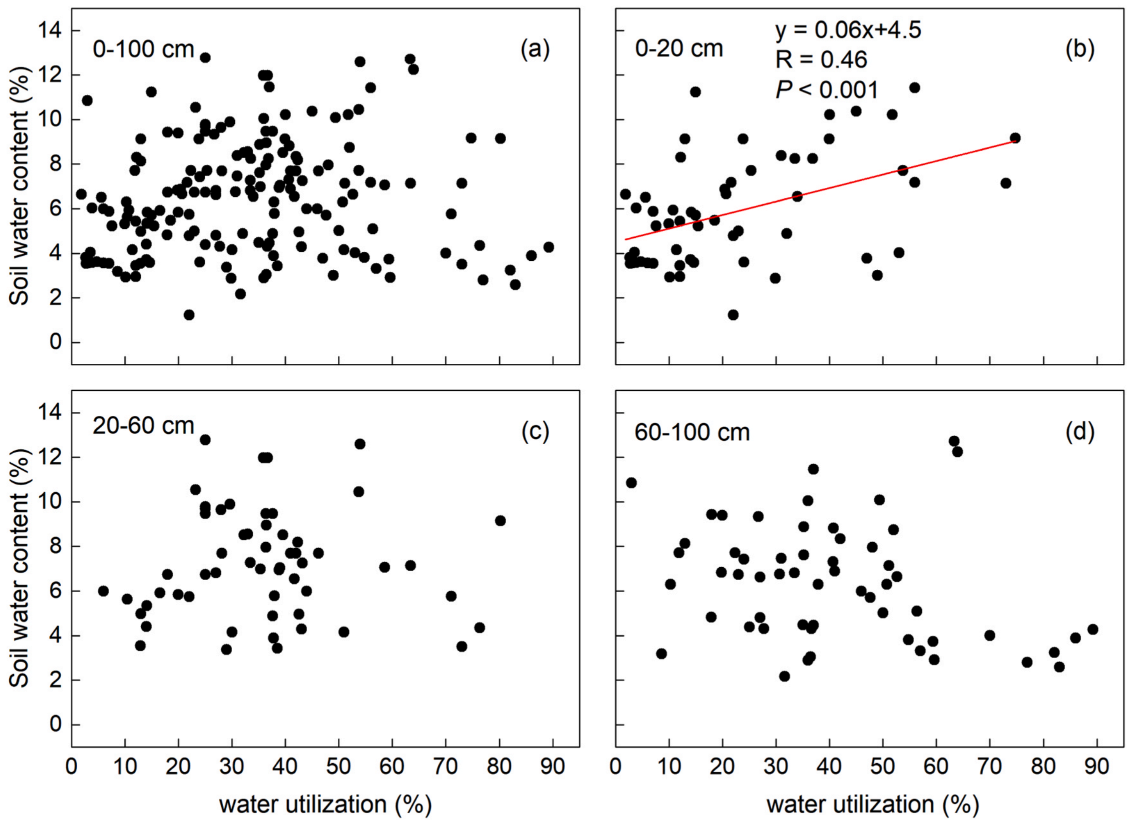

Fig. 6. Relationship between the contribution of water source and corresponding soil water content.

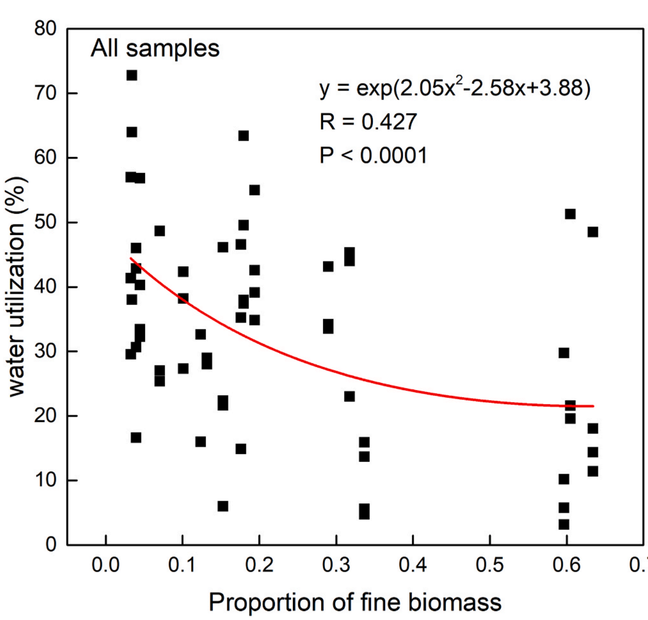

Fig. 7. Relationship between the contribution of water source and corresponding proportion of fine biomass.

water source apportionment better, due to consideration of the error structure (residual and process error) and the uncertainties of potential water sources (Brian and Brice, 2016; Parnell et al., 2010; Stock et al., 2018). Differences in the contribution from different layers of the 2 Bayesian mixing models may be attributed to the error parameterisation and posterior distribution in the model calculations. In this study, the performance of both Bayesian models was excellent, and the comprehensive performance of the MixSIR model was better. Therefore, the MixSIR model was employed to estimate the relative contributions of water sources in present study.

4.2. Analysis of water sources under the three treatments

The isotopic values of xylem water and soil water exhibited seasonal variations and between field management practices (Fig. 4; Table S2), indicating that the water used by trees from May to September may came from different soil water sources in the different treatments. The shallow and middle layers have relatively high water contents due to water supplied by winter irrigation and snow melt, during the LFE stage (Dai et al., 2015; Zhao et al., 2018b). The trees in CK did not use water from the shallow water source (5.6%), and instead depended on water from the deep water source (72.8%), this was attribute to low temperatures and water consumption (Table S3; Zhang et al., 2018), However, under the MF and MR they used more proportions of water from shallow layer, 10.2% and 18%, respectively, possibly because the mulching and creation of ridges and furrows increased the soil temperature and humidity (Fig. 3; Table S3; Gu et al., 2016), thereby enhancing root activity in shallow soil layer (Clarke et al., 2015). During BYF and FTM, the root growth was the fastest and the root activity was strong (Cao and He., 2013). The trees could flexibly use the water source of each soil layer. CK treatment mainly used the middle and deep soil water sources; increased precipitation did not increase the utilization of shallow water sources in BYF in2019, which may be because of a decrease in the soil water content in the shallow layer (compared with the other two treatment groups) due to water loss through evaporation (Table S3). Moreover, 74% of the precipitation events were < 5 mm, which is an invalid rainfall amount for crop growth (Zhao et al., 2018b), because of which, the root system sensitivity to precipitation was reduced. Only when the precipitation increases to a certain threshold, the root system in the shallow soil layer can respond, and the root system can form the ability to maintain absorption of shallow water source (Zhao et al., 2018b). In contrast, under MR and MF the mulching measures reduced the water loss from soil evaporation, and under MR, the tillage measures could sufficiently increase the infiltration of the precipitation to induce responses (Table S3; Liu et al., 2014). Compared to CK, the trees in MF and MR can flexibly switch to different water sources due to increased soil water content and root biomass in each soil layers. Increased absorption of shallow water sources in BYF 2019 may be because the ridges increased rainfall infiltration and thus induce strongly responses from rainfall in MR. In autumn, the temperature and wolfberry transpiration dropped, but rain was scarce, so both soil water content and root activity declined in the shallow layer, and wolfberry preferred use of water in the middle and deep soil layers, which is relatively abundant and stable (Gao et al., 2018a).

4.3. Impact of soil water availability and fine roots on water sources

Root water uptake is closely related to soil water availability and the distribution of functional roots (Kulmatiski et al., 2017; Gao et al., 2018a). We found that contributions of the shallow soil layer were positively correlated with its water content, indicating that the trees' root systems were sensitive to the shallow water sources and responded rapidly to changes (except CK), due to the high density of fine roots and possibly through changes in the activity or abundance of aquaporins (Gregory et al., 2015). The root systems of wolfberries may be able to exploit a large horizontal area of shallow soil, which may also facilitate absorption of nutrients that are generally highest in the shallow layer (Table 1, Clarke et al., 2015). Similar results were reported by Gao et al. (2018b), who revealed a positive correlation between the soil water content and root water uptake in a semiarid revegetated ecosystem. In the middle and deep soil layers, the trees' water utilisation did not match the soil water content. A possible explanation for this finding is that the trees' water requirements could be more easily met in the shallow layer, owing to the strong concentration of the trees' root in the shallow soil layer, soil water availability is not a major constraint factor in the trees' water absorption (Huo et al., 2020). We detected a non-linear correlation between FRLD and water source contributions, possibly because the decline in shallow water availability during the long drought in September (Fig. 5) led to more water uptake from the deep layer with low FRLD (Yang et al., 2018). Changes in the plants' water sources may also be related to the architecture and hydraulic effects of root systems (Rosado et al., 2011; Kulmatiski and Beard, 2013). Therefore, plants' water use strategies are inextricably linked to soil water availability and their fine root distributions.

4.4. Effect of field management practices on wolfberry yield and WUE

Studies have reported that both mulching and tillage measures can improve the yield and WUE in maize and wheat (Fang et al., 2021; Daryanto et al., 2017), mainly because mulching can increase the accumulation of soil water due to reduced soil evaporation and ridge–furrow farming practice can enhance the use of rainfall (Zhang et al., 2021). In addition, mulching and tillage measures can effectively increase surface soil moisture, soil temperature and water use. Such hydrothermal conditions play an important role in the dry matter accumulation and growth yield of plants (Zhang et al.,2021). Although the magnitude of the difference was small in evapotranspiration among the 3 treatments in 2018, the soil evaporation in MF and MR was less than that in CK (Table S3), indicating that more soil water in MF and MR was used for plant transpiration. Thus, the WUE in MF and MR was increased by 5% and 17% compared with that in CK.

Irrigation water is becoming scarce due to the increasing demands for water for industrial, urban and other uses in arid and semi-arid areas (Hamzei, 2011), and it is projected that global mean temperature rises by at least 2 ℃ by the end of the twenty-first century, particularly on TP (Chen et al., 2013). Hence, traditional flat planting (as in the CK treatment) may no longer be suitable for agriculture in many drylands, and in these areas water-conserving agricultural measures may be needed. We found that the soil water contents and proportional use of shallow and middle water sources were consistently higher under the MF and MR than those under CK treatments throughout the growth period. Shallow soil water is thus extremely important for wolfberry production. This is consistent with reports that a combination of full film mulching and tillage is an effective way to improve soil moisture and temperature (Mo et al., 2017; Liao et al.,2019b, 2021), with great potential for saving water in arid and semi-arid areas (Gu et al., 2016). In the context of rainfall increases on the TP (Kuang and Jiao, 2016), film mulching and tillage measures could collect large volumes of rainwater and increase the available water for plants, thereby increasing production and WUE. Therefore, we recommend it as a water management strategy for dryland wolfberry orchards.

5. Conclusion

Our analysis of Chinese wolfberry's water use patterns in different management practices using stable oxygen isotope techniques and three models (IsoSource, MixSIR and MixSIAR). No significant difference was noted in water utilisation predicted using the 3 methods in this study. The three models exhibited good performance for wolfberry water source apportionment, and the similar results acquired using the three models indicated that the prediction of wolfberry water source is reliable. Overall, the MixSIR model exhibited relatively better performance than the IsoSource and MixSIAR models. The CK trees tended to use more soil water from deeper layers, and their water use patterns were insensitive to rainfall, whereas the MF and MR trees shifted their water source between all three layers, depending on soil water content. The proportional contribution of only at shallow water layer was positively correlated with its water content, and overall contributions of the layers were exponentially decayed with FRLD in them. The water source utilisation of the MR trees was found to be highly flexible and sensitive to precipitation (irrigation) during the growth period, whereas tillage and film mulching were found to increase the shallow soil water content in the field, wolfberry's proportional use of shallow soil water, wolfberry yield and WUE. Therefore, it was established as the most effective water management practice in wolfberry orchards. Further study is however required to enhance the quantitative understanding of soil nutrients and subsurface irrigation to optimize the field management practices, such as irrigation schedules and modes.

Declaration of Competing Interest

The authors declare that they have no known competing financial interests or personal relationships that could have appeared to influence the work reported in this paper.

Acknowledgements

This work was jointly supported by the National Technology Research and Development Program key special projects of China (2017YFC0403600), the National Natural Science Foundation of China (41771316), the Integrative Science-Technology Innovation Engineering Project of Shaanxi (No. 2016KTZDNY-01-03), the 111 Project (No. B12007), and CAS "Youth Scholar of West China" Program (XAB2018A04). We appreciate the technical help from Jingjing Jin, Institute of Water-saving Agriculture in Arid Areas of China, Northwest A&F University.

Appendix A. Supporting information

Supplementary data associated with this article can be found in the online version at doi:10.1016/j.agwat.2021.107010.

References

Barbeta, A., Penuelas, J., 2017. Increasing carbon discrimination rates and depth of water uptake favor the growth of Mediterranean evergreen trees in the ecotone with temperate deciduous forests. Glob. Chang. Biol. 23 (12), 5040–5068.

Barbeta, A., Jones, S.P., Clavé, L., Wingate, L., Gimeno, T.E., Fréjaville, B., Wohl, S., Ogée, J., 2018. Hydrogen isotope fractionation affects the identification and quantification of tree water sources in a riparian forest. Hydrol. Earth Syst. 23 (4), 2129–2146.

Brian, S., Brice, S., 2016. MixSIAR GUI User Manual. Version 3.1. https://github.com/brianstock/MixSIAR/.

Cai, Y., Wu, P., Zhu, D., Zhang, L., Zhao, X., Gao, X., Ge, M., Song, X., Wu, Y., Dai, Z., 2021. Subsurface irrigation with ceramic emitters: An effective method to improve apple yield and irrigation water use efficiency in the semiarid Loess Plateau. Agric., Ecosyst. Environ. 313 (2021), 107404.

Cao, G., Tang, Y., Mo, W., Wang, Y., Li, Y., Zhao, X., 2004. Grazing intensity alters soil respiration in an alpine meadow on the Tibetan plateau. Soil Biol. Biochem. 36 (2), 237–243.

Cao, X., Yang, P., Engel, B.A., Li, P., 2018. The effects of rainfall and irrigation on cherry root water uptake under drip irrigation. Agric. Water Manag. 197, 9–18.

Cao, Y.L., He, J., 2013. *Lycium barbarum* L. cultivated science. Sunshine press, Yinchuan, pp. 24–26 (In Chinese).

Chen, H., Zhu, Q., Wu, N., Wang, Y., Peng, C.H., 2011. Delayed spring phenology on the Tibetan Plateau may also be attributable to other factors than winter and spring warming. Proc. Natl. Acad. Sci. U. S. A. 108 (19), 93.

Chen, H., Zhu, Q., Peng, C., Wu, N., Wang, Y.F., Fang, X.Q., Gao, Y.H., Zhu, D., Yang, G., Tian, J.Q., Kang, X.M., Piao, S.L., Ouyang, H., Xiang, W.H., Luo, Z.B., Jiang, H., Song, X.Z., Zhang, Y., Yu, G.R., Zhao, X.Q., Gong, P., Yao, T.D., Wu, J.H., 2013. The impacts of climate change and human activities on biogeochemical cycles on the Qinghai-Tibetan Plateau. Glob. Chang. Biol. 19 (10), 2940–2955.

Chen, X., Zhang, T., Guo, R., Li, H., Zhang, R., Degen, A.A., Huang, K., Wang, X., Bai, Y., Shang, Z., 2021. Fencing enclosure alters nitrogen distribution patterns and tradeoff strategies in an alpine meadow on the Qinghai-Tibetan Plateau. Catena 197, 104948.

Clarke, S.J., Lamont, K.J., Pan, H.Y., Barry, L.A., Hall, A., Rogiers, S.Y., 2015. Spring root-zone temperature regulates root growth, nutrient uptake and shoot growth dynamics in grapevines. Aust. J. Grape Wine R. 21 (3), 479–489.

Dai, Y., Zheng, X., Tang, L., Li, Y., 2015. Stable oxygen isotopes reveal distinct water use patterns of two Haloxylon species in the Gurbantonggut Desert. Plant Soil 389 (1–2), 73–87.

Daryanto, S., Wang, L., Jacinthe, P.-A., 2017. Can ridge-furrow plastic mulching replace irrigation in dryland wheat and maize cropping systems? Agric. Water Manag. 190, 1–5.

Dawson, T.E., Ehleringer, J.R., 1991. Streamside trees that do not use stream water. Nature 350 (6316), 335–337.

Dawson, T.E., Mambelli, S., Plamboeck, A.H., Templer, P.H., Tu, K.P., 2002. Stable isotopes in plant ecology. Annu. Rev. Ecol. Syst. 33 (2002), 507–559.

Deng, Y., Gou, X., Gao, L., Yang, M., Zhang, F., 2017. Spatiotemporal drought variability of the eastern Tibetan Plateau during the last millennium. Clim. Dyn. 49 (5–6), 2077–2091.

Ehleringer, J.R., Dawson, T.E., 1992. Water uptake by plants: perspectives from stable isotope composition. Plant Cell Environ. 15 (9), 1073–1082.

Ellsworth, P.Z., Williams, D.G., 2007. Hydrogen isotope fractionation during water uptake by woody xerophytes. Plant Soil 291 (1–2), 93–107.

Evaristo, J., McDonnell, J.J., Clemens, J., 2017. Plant source water apportionment using stable isotopes: a comparison of simple linear, two-compartment mixing model approaches. Hydrol. Process. 31 (21), 3750–3758.

Fang, H., Li, Y., Gu, X., Yu, M., Du, Y., Chen, P., Li, Y., 2021. Evapotranspiration partitioning, water use efficiency, and maize yield under different film mulching and nitrogen application in northwest China. Field Crops Res. 264 (264), 108103.

Feng, J., Wang, T., Qi, S., Xie, C., 2005. Land degradation in the source region of the Yellow River, northeast Qinghai-Xizang Plateau: classification and evaluation. Environ. Geol. 47 (4), 459–466.

Fu, B., Li, Z., Gao, X., Wu, L., Jian, L., Peng, W., 2021. Effects of subsurface drip irrigation on alfalfa (Medicago sativa L.) growth and soil microbial community structures in arid and semi-arid areas of northern China. Appl. Soil Ecol. 159 (2021), 103859.

Gao, X., Liu, Z., Zhao, X., Ling, Q., Huo, G., Wu, P., 2018a. Extreme natural drought enhances interspecific facilitation in semiarid agroforestry systems. Agric. Ecosyst. Environ. 265, 444–453.

Gao, X., Zhao, X., Li, H., Guo, L., Lv, T., Wu, P., 2018b. Exotic shrub species (*Caragana korshinskii*) is more resistant to extreme natural drought than native species (*Artemisia gmelinii*) in a semiarid revegetated ecosystem. Agr. For. Meteorol. 263, 207–216.

Gregory, V.D.H., Dambrine, E., Pollier, B., Zeller, B., Ranger, J., Legout, A., 2015. Mg and ca uptake by roots in relation to depth and allocation to aboveground tissues: results from an isotopic labeling study in a beech forest on base-poor soil. Biogeochemistry 122 (2–3), 375–393.

Grossiord, C., Sevanto, S., Dawson, T.E., Adams, H.D., Collins, A.D., Dickman, L.T., Newman, B.D., Stockton, E.A., McDowell, N.G., 2017. Warming combined with more extreme precipitation regimes modifies the water sources used by trees. New Phytol. 213 (2), 584–596.

Gu, X.B., Li, Y.N., Du, Y.D., 2016. Continuous ridges with film mulching improve soil water content, root growth, seed yield and water use efficiency of winter oilseed rape. Ind. Crop Prod. 85, 139–148.

Hamzei, J., 2011. Seed, oil, and protein yields of canola under combinations of irrigation and nitrogen application. Agron. J. 103 (4), 1152–1158.

Huo, G., Zhao, X., Gao, X., Wang, S., Pan, Y., 2018. Seasonal water use patterns of rainfed jujube trees in stands of different ages under semiarid plantations in China. Agric. Ecosyst. Environ. 265, 392–401.

Huo, G., Zhao, X., Gao, X., Wang, S., 2020. Seasonal effects of intercropping on tree water use strategies in semiarid plantations: evidence from natural and labelling stable isotopes. Plant Soil. 2020 (453), 229–243.

Jin, X., Jiang, P., Ma, D., Li, M., 2019. Land system evolution of Qinghai-Tibetan Plateau under various development strategies. Appl. Geogr. 104, 1–9.

Kuang, X., Jiao, J., 2016. Review on climate change on the tibetan plateau during the last half century. J. Geophys. Res. Atmos. 121 (8), 3979–4007.

Kulmatiski, A., Beard, K.H., 2013. Root niche partitioning among grasses, saplings, and trees measured using a tracer technique. Oecologia 171 (1), 25–37.

Kulmatiski, A., Adler, P.B., Stark, J.M., Tredennick, A.T., 2017. Water and nitrogen uptake are better associated with resource availability than root biomass. Ecosphere 8 (3), e1738.

Lei, C., Xiao, J., Shi, F., Guo, Y., Zhao, J., Zheng, L., 2020. Extraction methods of wolfberry plantation in qaidam region: a comparative study. Chin. Agric. Sci. Bull. 36 (17), 124–143 (In Chinese with English abstract).

Li, L., Gao, X., Wu, P., Zhao, X., Li, H., Ling, Q., Sun, W., 2017. Soil water content and root patterns in a rain-fed jujube plantation across stand ages on the Loess Plateau of China. Land Degrad. Dev. 28 (1), 207–216.

Li, Y., 2019. Water and fertilizer coupling technology model boosts Qaidam wolfberry industry to improve quality and efficiency. Agric. Technol. 39, 13 (In Chinese with English abstract).

Liao, R.K., Wu, W.Y., Hu, Y.Q., Hun, Y., 2019a. Quantifying moisture availability in soil profiles of cherry orchards under different irrigation regimes. Agric. Water Manag. 225 (2019), 105780.

Liao, R.K., Wu, W.Y., Hu, Y.Q., Huang, Q.N., Yan, H., 2019b. Micro-irrigation strategies to improve water-use efficiency of cherry trees in Northern China. Agric. Water Manag. 221, 388–396.

Liao, Y., Cao, H.X., Xue, W.K., Liu, X., 2021. Effects of the combination of mulching and deficit irrigation on the soil water and heat, growth and productivity of apples. Agric. Water Manag. 243 (2021), 106482.

Lin, G., Sternberg, L.D.S.L., 1993. Hydrogen isotopic fractionation by plant roots during water uptake in coastal wetland plants. In Stable Isotopes and Plant Carbon-water Relations. Academic Press, San Diego, CA, USA, pp. 497–510.

Liu, X., Li, X., Hai, L., Wang, Y., Li, F., 2014. How efficient is film fully-mulched ridge–furrow cropping to conserve rainfall in soil at a rainfed site? Field Crop Res. 169, 107–115.

Miehe, G., Schleuss, P.M., Seeber, E., Babel, W., Biermann, T., Braendle, M., Chen, F.H., Coners, H., Foken, T., Gerken, T., Graf, H.F., Guggenberger, G., Hafner, S., Holzapfel, M., Ingrisch, J., Kuzyakov, Y., Lai, Z.P., Lehnert, L., Leuschner, C., Li, X. G., Liu, J.Q., Liu, S.B., Ma, Y.M., Miehe, S., Mosbrugger, V., Noltie, H.J., Schmidt, J., Spielvogel, S., Unteregelsbacher, S., Wang, Y., Willinghofer, S., Xu, X.L., Yang, Y.P., Zhang, S.R., Opgenoorth, L., Wesche, K., 2019. The Kobresia pygmaea ecosystem of the Tibetan highlands - origin, functioning and degradation of the world's largest pastoral alpine ecosystem Kobresia pastures of Tibet. Sci. Total Environ. 648, 754–771.

Miehe, G.M.S., Will, M., Opgenoorth, L., Duo, L., Dorgeh, T., Liu, J., 2008. An inventory of forest relicts in the pastures of Southern Tibet (Xizang A.R., China). Plant Ecol. 194 (2), 157–177.

Mo, F., Wang, J.Y., Zhou, H., Luo, C.L., Zhang, X.F., Li, X.Y., Li, F.M., Xiong, L.B., Kavagi, L., Nguluu, S.N., Xiong, Y.C., 2017. Ridge-furrow plastic-mulching with balanced fertilization in rainfed maize (*Zea mays* L.): An adaptive management in east African Plateau. Agr. For. Meteorol. 236, 100–112.

Parnell, A.C., Inger, R., Bearhop, S., Jackson, A.L., 2010. Source partitioning using stable isotopes: coping with too much variation. Plos One 5 (3), 9672.

Phillips, D.L., Gregg, J.W., 2003. Source partitioning using stable isotopes: coping with too many sources. Oecologia 136 (2), 261–269.

Rosado, B.H.P., Martins, A.C., Colomeu, T.C., OLIveira, R.S., Joly, C.A., Aidar, M.P.M., 2011. Fine root biomass and root length density in a lowland and a montane tropical rain forest, SP, Brazil. Biota Neotrop. 11 (3), 203–209.

Rothfuss, Y., Javaux, M., 2017. Reviews and syntheses: Isotopic approaches to quantify root water uptake: a review and comparison of methods. Biogeosciences 14, 2199–2224.

Stock, B.C., Jackson, A.L., Ward, E.J., Parnell, A.C., Phillips, D.L., Semmens, B.X., 2018. Analyzing mixing systems using a new generation of Bayesian tracer mixing models. PeerJ 6, 5096.

Wang, J., Lu, N., Fu, B., 2019. Inter-comparison of stable isotope mixing models for determining plant water source partitioning. Sci. Total Environ. 666, 685–693.

Wang, J., Gao, X., Zhou, Y., Wu, P., Zhao, X., 2020a. Impact of conservation practices on soil hydrothermal properties and crop water use efficiency in a dry agricultural region of the tibetan plateau. Soil Tillage Res. 200, 104619.

Wang, S., An, J., Zhao, X., Gao, X., Wu, P., Huo, G., Robinson, B., 2020b. Age- and climate- related water use patterns of apple trees on China's Loess Plateau. J. Hydrol. 582, 124462.

Wu, H., Li, X., Li, J., Jiang, Z., Chen, H., Ma, Y., Huang, Y., 2016. Differential soil moisture pulse uptake by coexisting plants in an alpine Achnatherum splendens grassland community. Environ. Earth Sci. 75 (10), 914.

Wu, J., Li, M., Zhang, X., Fiedler, S., Gao, Q., Zhou, Y., Cao, W., Hassan, W., Mărgărint, M.C., Tarolli, P., Tietjen, B., 2021. Disentangling climatic and anthropogenic contributions to nonlinear dynamics of alpine grassland productivity on the Qinghai-Tibetan Plateau. J. Environ. Manag. 281 (2021), 111875.

Wu, Y., Du, T., Yuan, Y., Shukla, M., 2018. Stable isotope measurements show increases in corn water use efficiency under deficit irrigation. Sci. Rep. 8 (1), 14113.

Xu, M., Kang, S., Wang, X., Pepin, N., Wu, H., 2019. Understanding changes in the water budget driven by climate change in cryospheric-dominated watershed of the northeast Tibetan Plateau, China. Hydrol. Process. 33 (7), 1040–1058.
Yang, B., Wen, X., Sun, X., 2015. Seasonal variations in depth of water uptake for a subtropical coniferous plantation subjected to drought in an East Asian monsoon region. Agric. . Meteorol. 201, 218–228.
Yang, B., Wang, P., You, D., Liu, W., 2018. Coupling evapotranspiration partitioning with root water uptake to identify the water consumption characteristics of winter wheat: a case study in the North China Plain. Agric. . Meteorol. 259, 296–304.
Yao, T., Thompson, L.G., Mosbrugger, V., Zhang, F., Ma, Y., Luo, T., Xu, B., Yang, X., Joswiak, D.R., Wang, W., Joswiak, M.E., Devkota, L.P., Tayal, S., Jilani, R., Fayziev, R., 2012. Third Pole environment (TPE). Environ. Dev. 3, 52–64.
Zhang, G.X., Mo, F., Shah, F., Meng, W.H., Liao, Y.C., Han, J., 2021. Ridge-furrow configuration significantly improves soil water availability, crop water use efficiency, and grain yield in dryland agroecosystems of the Loess Plateau. Agric. Water Manag. 245 (2021), 106657.
Zhang, J., Wang, N., Niu, Z., Sun, J., Dong, C., Zhang, L., 2018. Stable isotope analysis of water sources for Tamarix laxa in the mega-dunes of the Badain Jaran Desert. China J. Arid Land 10 (6), 821–832.
Zhang, Y., Zhang, M.J., Wang, S.J., Guo, R., Che, C.W., Du, Q.Q., Ma, Z., Su P. Y, Z., 2020. Comparison of different methods for determining plant water sources based on stable oxygen. Chin. J. Ecol. 39 (04), 1356–1368 (In Chinese with English abstract).
Zhao, L., Wang, L., Cernusak, L.A., Liu, X., Xiao, H., Zhou, M., Zhang, S., 2016. Significant difference in hydrogen isotope composition between xylem and tissue water in Populus Euphratica. Plant Cell Environ. 39 (8), 1848–1857.
Zhao, X., Li, F., Ai, Z., Li, J., Gu, C., 2018a. Stable isotope evidences for identifying crop water uptake in a typical winter wheat–summer maize rotation field in the North China Plain. Sci. Total Environ. 618, 121–131.
Zhao, X., Li, N., Gao, X., Huo, G., Pan, Y., 2018b. Characteristics of soil water utilization for different stand ages of jujube trees based on^{18}O tracking. Trans. Chin. Soc. Agr. Eng. 34 (3), 135–142 (In Chinese with English abstract).
Zhou, X., Wang, R.S., Gao, F., Xiao, H.J., Xu, H.S., Wang, D.M., 2019. Apple and maize physiological characteristics and water-use efficiency in an alley cropping system under water and fertilizer coupling in Loess Plateau, China. Agric. Water Manag. 221, 1–12.